8

Research Article

Xie Dongbai, Hong Hao, Duo Shuwang*, and Li Qiang

Application on oxidation behavior of metallic copper in fire investigation

https://doi.org/10.1515/htmp-2022-0014 received October 11, 2021; accepted December 19, 2021

Abstract: In fire investigations, the most important aspect is determining the presence of a liquid accelerant at the fire scene. The presence or absence of accelerants is critical evidence during trials for fire cases. Upon exposure to high temperatures, metallic substances undergo oxidation, which can be imparted by accelerants in the fire. Oxides and substrates found on metal surfaces offer valuable information on the characteristics of fire, including exposure temperature, duration, and involvement of a liquid accelerant. In this study, we investigated the oxidation behavior of copper at high temperatures in a simulated flame environment using ethanol combustion. After oxidation, the morphological, oxide phase composition, and microstructural features of specimens were characterized by observation, X-ray diffraction, X-ray photoelectron energy spectroscopy, transmission electron microscopy, and scanning electron microscopy with energy-dispersive spectroscopic analysis. The elemental carbon with a hexagonal structure deposited on the sample's surface was found, which may be incomplete combustion and the chemical composition of ethanol. Copper has a preferred orientation of oxide on the (111) crystal plane, which differs from oxidation in ordinary hot air that is related to the large Coulomb force of the (111) crystal plane. Hot air convection due to combustion may cause large areas of oxide layer on the copper surface to crack and peel. Oxide properties and surface state of metals strongly depended on oxidation duration, temperature, and atmosphere. These data shall offer reference

information for determining the presence of combustion accelerants at fire scenes.

Keywords: copper, surface oxidation, carbon, accelerant, fire investigation

1 Introduction

In court trials for fire cases, it is necessary to give scientific evidence. Usually, in order to attain the purpose of rapid arson, arsonists will choose to use liquid accelerants [1,2]. Thus, determining the presence of a fire accelerant at the scene is key to the court trial [2-4]. Currently, it is the most widely used method to identify accelerants in the fire scene; the first step is extracting suspicious accelerants fragments from fire debris (such as extraction, physical adsorption, distillation method, and chemical derivatization) [5–7], and then the chemical analysis was used to identify whether there were accelerant components in the specimen (such as gas chromatography-mass spectrometry, infrared, and ultraviolet) [8,9]. However, at the fire scene, the complex combustion environment and destruction during fire extinguishing make it not only difficult to extract quality samples for analysis but even more difficult to extract volatile combustion accelerants [4,10]. According to the high-temperature oxidation theory, when metals are oxidized in a fire, the oxidation product will record information about the temperature (combustion temperature), atmospheric composition (accelerants), and oxidation time (combustion duration). For example, unstable high temperature from flame combustion affects nucleation and growth of metal oxides; carbon from incomplete combustion is deposited on metal surfaces; plasma in the flame greatly accelerates metal oxidation and the air convection due to turbulence tears the metal oxide layer [11,12]. We proposed a new method of determining the presence of fire accelerants based on oxidation characteristics of metal, which may enhance evidence gathering for fire cases [13–17]. In this study, we used copper, one of the most common household metals, and ethanol which is also

e-mail: hhong94@foxmail.com

Xie Dongbai, Li Qiang: Faculty of Electro-Machical Information, Weifang University of Science and Technology, Shouguang 262700, China

Hong Hao: Jiangxi Key Laboratory of Materials Surface Engineering, Jiangxi Science and Technology Normal University, Nanchang 330013, China

^{*} Corresponding author: Duo Shuwang, Jiangxi Key Laboratory of Materials Surface Engineering, Jiangxi Science and Technology Normal University, Nanchang 330013, China,

widely used in fuels. This research will study the oxidation behavior of copper in a fire scene with ethanol as accelerants, aiming to offer complimentary insight into fire characteristics such as whether a liquid accelerant is involved. (XRD), Thermo Scientific K-Alpha + X-ray photoelectron energy Spectroscopy (XPS), and FEI-G2200 transmission electron microscope (TEM) were used to analyze the composition and phase of the sample.

2 Methods

In this study, copper (wt%), a widespread metal (Table 1) was used. The sample was cut into $3 \text{ mm} \times 10 \text{ mm} \times 20 \text{ mm}$ pieces and a 2 mm diameter hole was punched at the top. The surface was polished using SiC water sandpaper to 2000#. It was then mechanically polished and degreased using acetone, followed by ultrasonic cleaning and flushing with absolute ethanol before being dried with cold air for later use. The experiment simulated atmospheric oxidation during ordinary indoor fire using ethanol as a simulated accelerant. The simulation device is shown in Figure 1. Oxidation was evaluated after 0.5, 1, 2, 3, 4, 5, 10, 20, and 30 min and the temperature curve at each time point was plotted (Figure 2), through which the oxidation parameters were chosen based on actual oxidation conditions at the fire scene. After oxidation was completed, specimens were weighed and the surface was analyzed after surface oxides had naturally fallen off. Zeiss Sigma scanning electron microscopy (SEM) was used to examine the morphology of the oxidized sample. Oxford INCA energy-dispersive spectroscope (EDS), Shimadzu XRD-6100 X-ray diffractometer

Table 1: Chemical composition of copper (wt%)

Cu	0	Impurity
99.90-99.95	0.003-0.03	<0.1

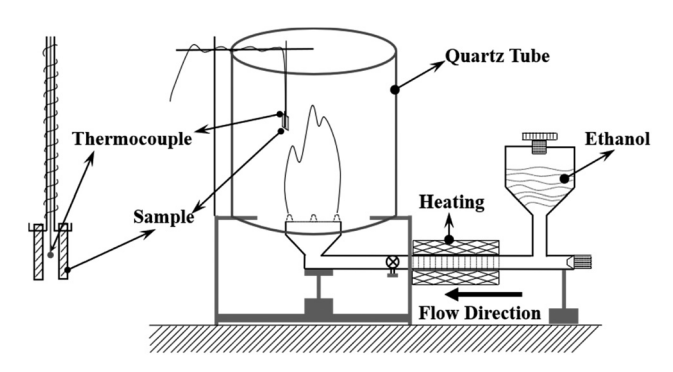


Figure 1: Ethanol combustion atmosphere simulation device.

3 Results

The oxide layer generated in the sample in this oxidation mode was not protective. After oxidation was complete, a large area of the oxide layer sample's surface was shed. In addition, repeated weight gain and loss occurred (Figure 3). Studies show that large volume changes between CuO/Cu₂O and Cu during oxidation [18] easily cause internal stress that causes the oxide layer to fall off easily. The substrate below the oxide layer was exposed to the combustion atmosphere and continued to oxidize, resulting in slight weight gain. When this cycle was repeated multiple times, the sample may not exhibit weight gain as it may enter a catastrophic oxidation state of weight loss.

The XRD results showed that the oxide layer was mainly composed of Cu₂O and CuO (Figure 4). Copper matrix peak analysis suggested that the oxide layer was very thin or the oxide layer peeled off, exposing fresh copper matrix which was consistent with the quality change analysis result (Figure 3). When copper was oxidized in the air, the intensity of the diffraction peak of the (311) crystal plane was much higher relative to the (111) crystal plane [11]. However, when oxidized under ethanol combustion, the diffraction intensity of the (111) crystal plane exceeded that of the (311) crystal plane, possibly because copper had a face-centered cubic structure and its (111) crystal plane was closely packed, its high atomic stacking density generated high Coulomb forces [19]. During oxidation, the (111) crystal plane exhibited relatively good adhesion when the oxide film fell off due to internal stress and convection caused by combustion. The XRD pattern showed that the intensity of the (111) crystal plane was higher relative to that of the (311) crystal plane.

There was no obvious oxidation on the sample surface after 0.5 min oxidation (Figure 5a). However, after oxidation for 1 min, the surface of the sample appeared to fall off. Increased oxidation was time-correlated with greater falling off of the oxide layer (Figure 5b and c). A non-shedding oxide layer was also present, generating a crisscross network structure (Figure 5c). Sections, where the oxide layer had fallen off, were characterized by granular protrusions, probably due to nucleation and growth

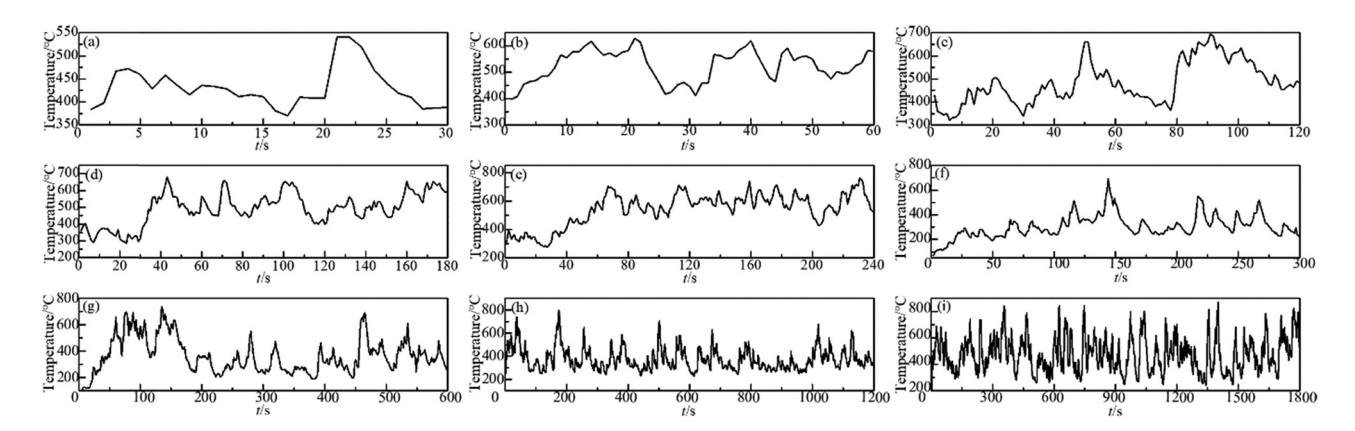


Figure 2: Temperature curve of oxidation for (a) 0.5 min, (b) 1 min, (c) 2 min, (d) 3 min, (d) 4 min, (e) 5 min, (f) 10 min, (h) 20 min, and (i) 30 min.

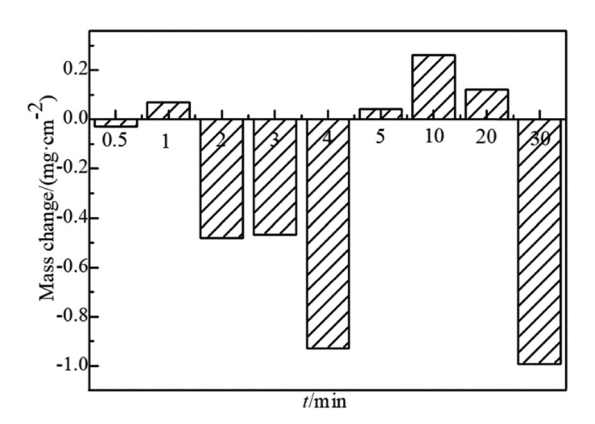


Figure 3: Sample mass change.

of copper oxide crystal grains. The oxide layer results from the growth of a fusion of these grains, further evidence can be obtained from Figure 5d. The non-shedding area has a loose and porous network structure. Sections of the sample surface from which the oxide layer had

fallen off-exhibit apparent nucleation and growth. EDS analysis revealed cube-shaped crystal grains, indicating that the atomic ratio of O:Cu was about 0.6 and that the crystal grains were mainly Cu₂O, with a tendency to transition to CuO, and the results of non-cubic crystal grains revealed an O:Cu atomic ratio of 0.1-0.2, indicating that the region was further oxidized after the oxide layer falls off. Analysis of the sample's surface morphology after oxidation for 4 min revealed a three-layer structure and that the outermost layer was a porous network oxide (Figure 5e). EDS analysis revealed an O:Cu atomic ratio of about 1, indicating that the outermost oxide was CuO. In Figure 5e, the intermediate layer was presumed to result from the oxide layer incompletely peeling off, hence separation from the CuO layer. EDS analysis revealed an O:Cu atomic ratio of about 0.5, indicating a Cu₂O layer. Volume differences due to internal attraction between the two oxides may have caused a separation of the oxide layers. The bottom layer was similar to Figure 5c and d. After the oxide layer had fallen, the matrix began to oxidize,

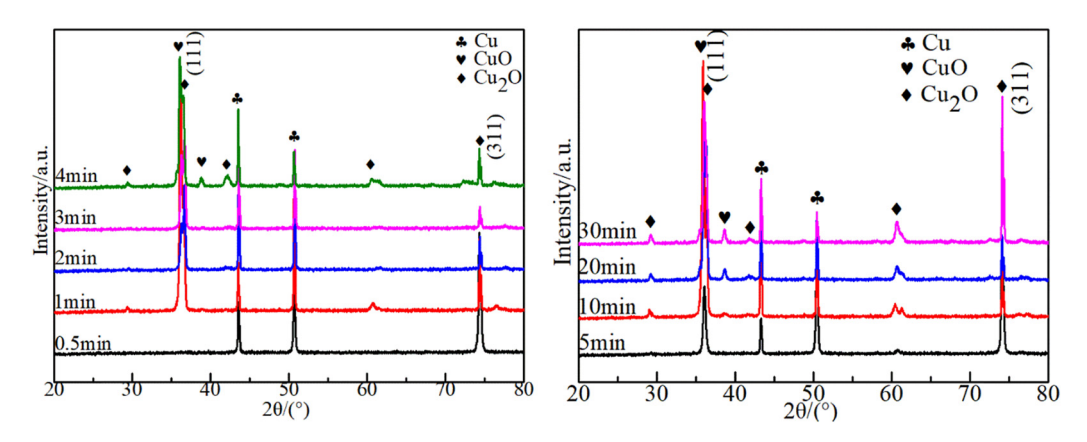


Figure 4: Results of copper surface XRD analysis in an ethanol combustion atmosphere.

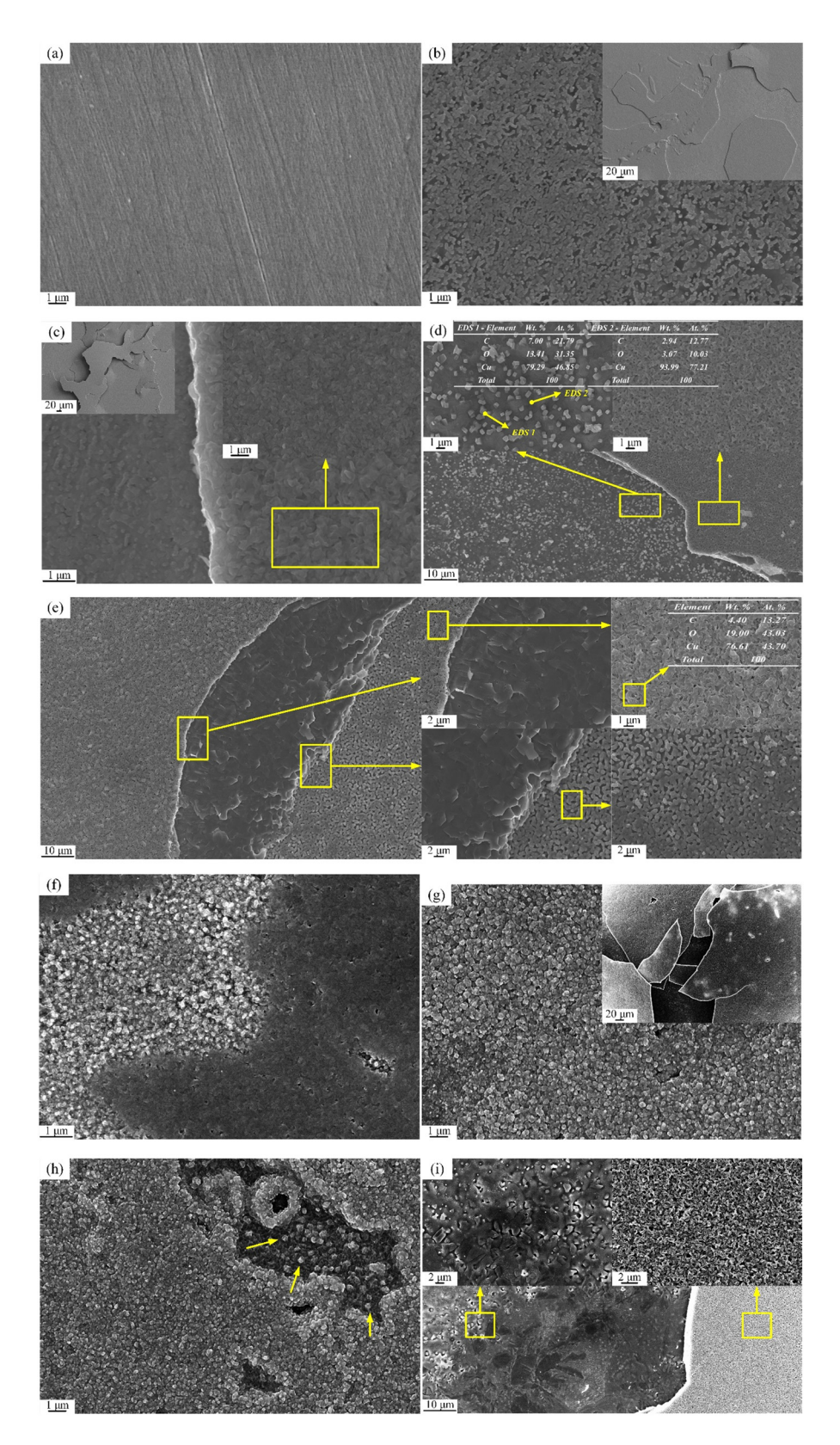


Figure 5: SEM surface morphology of the copper samples after oxidation at (a) 0.5 min, (b) 1 min, (c) 2 min, (d) 3 min, (e) 4 min, (f) 5 min, (g) 10 min, (h) 20 min, and (i) 30 min.

leading to obvious crystal grain growth, contiguousness, and expansion. The low content of oxygen atoms of crystal grain showed that in the initial stage of oxidation. The oxide layer was mainly comprised of Cu₂O and CuO. Because the outermost oxygen potential was high, CuO occurred in the outer layer, and Cu₂O was in the inner layer, corresponding to the O:Cu atomic ratio seen in the EDS results. Extending oxidation time to 5 and 10 min significantly increased the extent of oxide layer shedding, with oxidation entering catastrophic oxidation. From the mark in Figure 5h, it can be seen the growth of the crystal grains, and from the comparison between the oxide scale and the matrix in Figure 5i, it can be seen that the oxidation process has cyclically occurred in between the steps of "oxidation, oxide layer shedding, re-oxidation" which was consistent with the mass analysis results (Figure 3). About 15-20% carbon was deposited on the sample surface, possibly from incomplete combustion of the accelerant.

To determine the carbon structure of the oxide layer more accurately, the peeled oxide scale was further observed by TEM (Figure 6). This analysis found that elemental carbon with a spatial point group of P63/mmc was formed in the oxide layer, which had a hexagonal structure with a Miller index of a = b = 2.522 Å, c = 8.237 Å, $\alpha = \beta = 90^{\circ}$, $\gamma = 120^{\circ}$ [20]. There were eight atoms in a unit cell that fell into two atom types: four occupying the

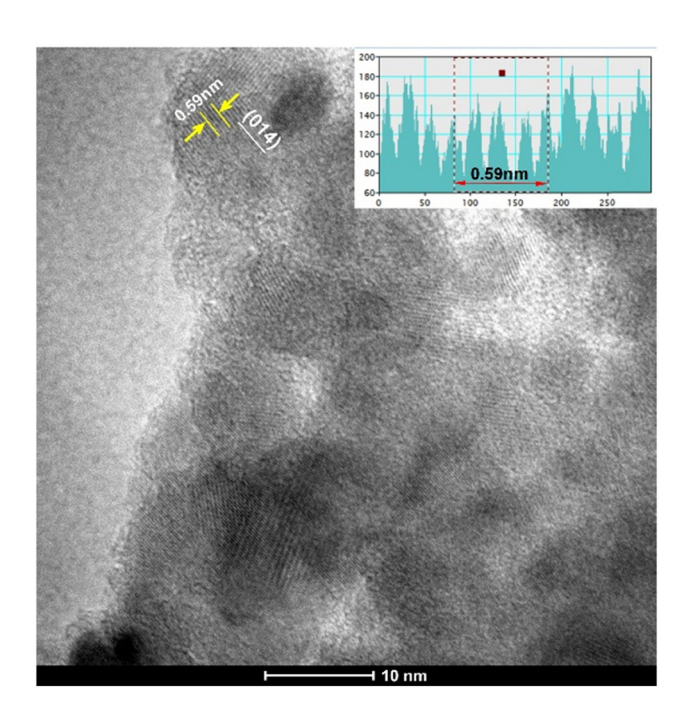


Figure 6: Results from TEM analysis of copper oxide scale after oxidation in an ethanol combustion environment.

e-point of the space group and four occupying the f-point of the space group. The atoms were arranged in a stacking configuration of AaBbCcBb/AaBbCcBb/Aa.

The XPS analysis showed that the main components of the oxide layer were Cu, C, and O (Figure 7). Cu was present as Cu(I) and Cu(II), which was consistent with XRD and SEM results. O mainly existed in the form of metal oxides and C-O, and C=O, which directly correlates to ethanol composition. C was present in a typical chemical state of C-C, CO, and C=O. Along with TEM results, these data show that in the combustion atmosphere of ethanol, high-temperature ethanol cracking caused some carbon to form an organic carbon ring with a hexagonal structure. The other part of carbon existed in the oxide layer in the form of C-O, and C=O. The carbon deposited in the copper oxide layer directly correlated to the composition of ethanol (the accelerant).

4 Discussion

Copper oxidation during ethanol combustion differed from its air oxidation in the following ways: (1) the oxidizing atmosphere generated by ethanol combustion promoted metal oxidation, (2) hot air convection around the sample due to flame combustion promoted peeling of the oxide layer, (3) elemental carbon produced by incomplete ethanol combustion was deposited on the metal surface.

During copper oxidation, the decisive factor in oxide layer formation was the outward diffusion of copper ions [18,21]. When copper ions diffuse outward, they leave a vacancy that diffuses into the interior in two possible ways. One, the diffusion may be smooth, with the copper ions being outwards and the vacancies inwards. As oxidation progressed, the oxide layer continued to thicken and formed a protective oxide layer. However, in actual metal materials, various defects hinder the vacancy movement. The other was, vacancies may gather at the interface between the oxide layer and the substrate until macroscopic defects such as holes were formed when diffusion encountered resistance. There were two situations where the holes existed. One, the oxide layer may collapse to fill the hole, causing local stress to cause the oxide layer to fall off, and the collapse return to its original state. The other was that the oxide layer does not collapse and the hole was not filled. Alternatively, the oxide layer may incompletely collapse, leaving some holes that block the channel for copper ions to diffuse out. Thereby, the internal stress in the oxide layer was not be released. As oxidation progressed, internal stress

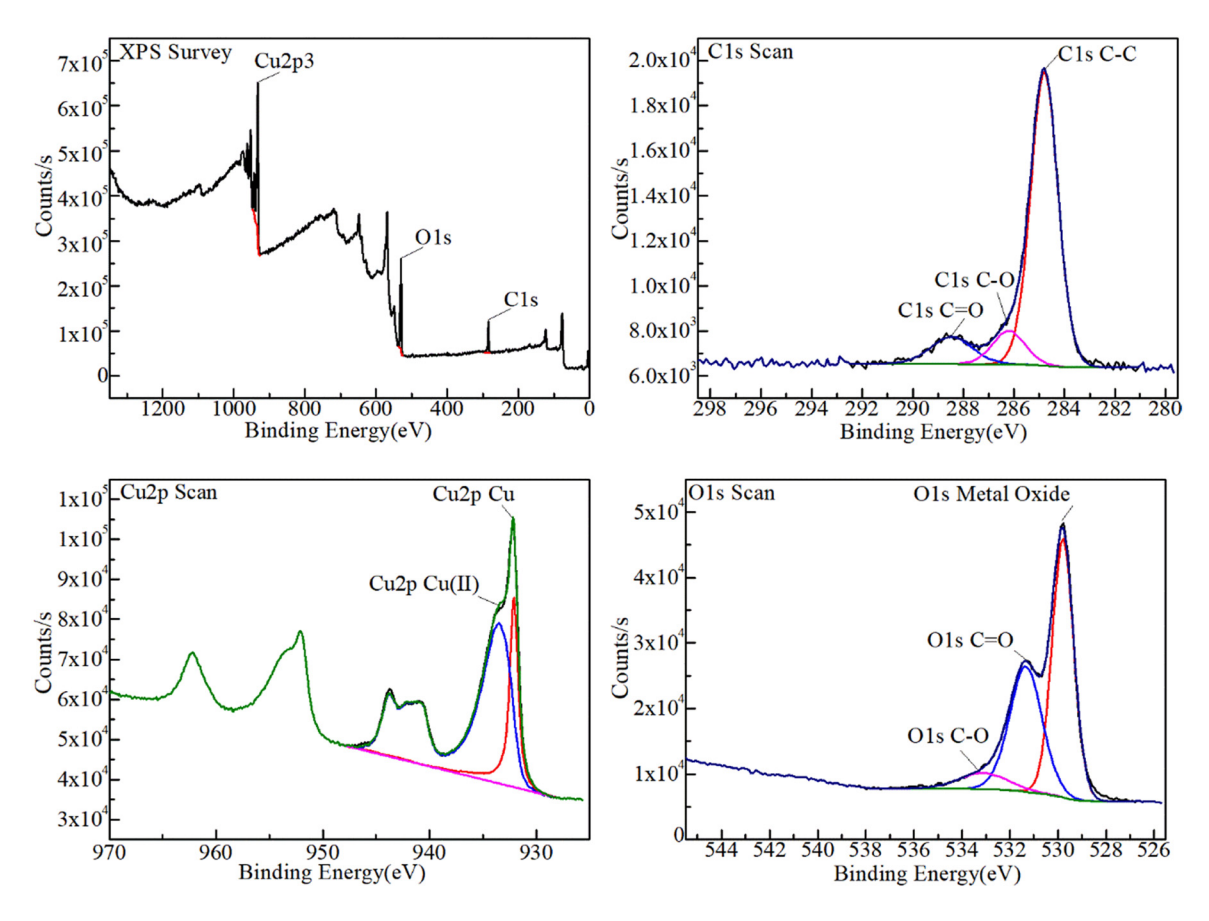


Figure 7: Results from XPS analysis of the oxide layer that peeled off during oxidation.

accumulation caused cracks in the oxide layer. Another important factor that affected copper oxide layer formation was the Pilling-Bedworth ratio (PBR ratio), which refers to the ratio between the oxide volume produced by the metal during oxidation and the metal volume consumed. The PBR of Cu₂O and CuO were 1.64 and 1.7, respectively [22]. When the PBR value was greater than 1, the oxide layer will form compressive stress, which may cause it to crack. Cu₂O/CuO has poor toughness and low-stress release ability, worsening oxide layer cracking. Here, the convection of hot air caused by flame combustion may have caused the tearing of an already cracked oxide layer. This was consistent with the many cracked oxide films observed in SEM analysis. Because the copper (111) crystal plane was a close-packed surface of a face-centered cubic crystal, its high atomic stacking density generated high Coulomb forces. During tearing of the oxide layer by hot airflow, the (111) crystal plane possessed a large Coulomb force, hence a large amount of (111) crystal plane oxide existed after the oxidation was complete. This also illustrated the difference in the content of (111) crystal planes and (311) crystal planes in the XRD results and hot air.

In addition to the high temperature that oxidizes metal in an ethanol combustion environment, H_2O and CO_2 enhance copper oxidation. The reaction mechanism of ethanol in the combustion process is represented by the reactions below [23–26]

$$O_2 + h\nu \rightarrow 20^\circ$$
, (1)

$$C_2H_6 O \rightarrow C_2H_4 + H_2O,$$
 (2)

$$C_2H_4 \rightarrow 2 C + 2H_2,$$
 (3)

$$H_2 + O^{\circ} \to H_2O,$$
 (4)

$$C + O^{\circ} \rightarrow CO$$
, (5)

$$2CO + O_2 \rightarrow CO_2$$
, (6)

 O° = free oxygen atom, hv = energy.

An alcohol cracking reaction occurs during ethanol combustion, with the generated carbon being deposited on the metal surface, which was consistent with EDS and TEM results. The structure of elemental carbon generated on the sample surface may correspond to the type of metal oxide, the type of combustion accelerant, and oxidation temperature. Studies have shown that metal oxides can catalyze carbon into carbon nanotubes/carbon

fibers [27–29]. Thus, studying the form of carbon in the oxide layer was expected to reverse deduce the fire environment, uncovering evidence for court cases. The H₂O, CO₂, and other components generated by combustion accelerated copper oxidation or formed an oxidation system with other components to accelerate copper oxidation (Reaction (7)-(8)) [30,31]:

$$2Cu + H_2O = Cu_2O + H_2, (7)$$

$$2Cu + H_2O + CO_2 + O_2 = Cu_2(OH)_2CO_3.$$
 (8)

Of these, $Cu_2(OH)_2CO_3$ is a volatile product [30]. The H₂ generated by copper and water vapor accelerated the formation and cracking of oxide layers. Since outward copper ion transmission was a regulatory step in metallic copper oxidation, and the Cu₂O, which accounts for most of the oxide layer, is a metal-deficient P-type semiconductor [11,30] with high ion vacancy concentration and low resistivity, it was impossible to prevent copper ions from diffusing outwards leading to continuous oxidation. The finding that copper metal undergoes catastrophic oxidation under the complex environmental conditions of ethanol combustion, and has characteristics that differ from hot air oxidation, offers a novel avenue for fire investigation.

5 Conclusion

In this study, the oxidation behavior of metal copper in the ethanol combustion environment has been studied. and its relationship with the accelerant in the fire scene has been clarified, which was expected to provide new ideas for fire investigations. Based on the results, these conclusions can be made:

- 1. Large-area cracking and peeling of the oxide layer appeared on the surface of the metal is related to the strong oxidizing gas components generated during oxidation, and the hot air convection resulting from combustion that tears the oxide layer.
- 2. The oxides generated on the (111) crystal plane of copper are far more than those generated on the (311) crystal plane, which is contrary to the results of oxidation via hot air. Because the copper (111) crystal plane is a close-packed surface of a face-centered cubic crystal, its high atomic stacking density generates high Coulomb forces. The large Coulomb force can maintain good oxide adhesion when the hot air convection caused by combustion tears the oxide layer.
- 3. Carbon element is deposited on the surface of metallic copper, which has a hexagonal structure that corresponds

to the chemical composition of ethanol (combustion accelerants).

Acknowledgments: The authors would like to thank the financial supports of the Startup Foundation for Doctors of Weifang University of Science and Technology and funded by the Key Laboratory of Impression Evidence Examination and Identification Technology, Ministry of Public Security, People's Republic of China (No. 2019). This work is also partially the Open-fund Project of Jiangxi Key Laboratory of Materials Surface Engineering (No. 2021CLKF002).

Funding information: Weifang University of Science and Technology and funded by the Key Laboratory of Impression Evidence Examination and Identification Technology, Ministry of Public Security, People's Republic of China (No. 2019). This work is also partially the Open-fund Project of Jiangxi Key Laboratory of Materials Surface Engineering (No. 2021CLKF002).

Author contribution: Xie Dongbai and Duo Shuwang contributed to the conception of the study; Hong Hao performed the experiment; Xie Dongbai and Duo Shuwang contributed significantly to analysis and manuscript preparation; Xie Dongbai and Hong Hao performed the data analyses and wrote the manuscript; Li Qiang helped perform the analysis with constructive discussions.

Conflict of interest: Authors state no conflict of interest.

Data availability statement: The datasets generated during and/or analysed during the current study are available from the corresponding author on reasonable request.

References

- Stauffer, E. and D. Byron. Alternative fuels in fire debris analysis: Biodiesel basics. Journal of Forensic Sciences, Vol. 52, No. 2, 2007, pp. 371-379.
- Falatová, B., M. Ferreiro-González, C. Martín-Alberca, D. Kačíková, Š. Galla, M. Palma, et al. Effects of fire suppression agents and weathering in the analysis of fire debris by HS-MS eNose. Sensors, Vol. 18, No. 6, 2018, id. 1933.
- Henneberg, M. L. and N. R. Morling. Unconfirmed [3] accelerants: Controversial evidence in fire investigations. The International Journal of Evidence & Proof, Vol. 22, No. 1, 2017, pp. 45-67.
- Dhabbah, A. M., S. S. Al-Jaber, A. H. Al-Ghamdi, and A. Agel. Determination of gasoline residues on carpets by

- SPME-GC-MS technique. Arabian Journal for Science and Engineering, Vol. 39, No. 9, 2014, pp. 6749-6756.
- [5] Baechler, S., S. Comment, and O. Delémont. Extraction and concentration of vapors from fire debris for forensic purposes: Evaluation of the use of radiello passive air sampler. Talanta, Vol. 82, No. 4, 2010, pp. 1247-1253.
- Borusiewicz, R., G. Zadora, and J. Zieba-Palus. Application of headspace analysis with passive adsorption for forensic purpose in the automated thermal desorption-gas chromatography-mass spectrometry system. Chromatographia, Vol. 60, No. 1, 2004, pp. S133-S142.
- Borusiewicz, R., J. Zieba-Palus, and G. Zadora. The influence of the type of accelerant, type of burned material, time of burning and availability of air on the possibility of detection of accelerants traces. Forensic Science International, Vol. 160, No. 2-3, 2006, pp. 115-126.
- [8] Tan, B., J. K. Hardy, and R. E. Snavely. Accelerant classification by gas chromatography/mass spectrometry and multivariate pattern recognition. Analytica Chimica Acta, Vol. 422, No. 1, 2000, pp. 37-46.
- Lu, Y., P. Chen, and P. B. Harrington. Comparison of differential mobility spectrometry and mass spectrometry for gas chromatographic detection of ignitable liquids from fire debris using projected difference resolution. Analytical and Bioanalytical Chemistry, Vol. 394, No. 8, 2009, pp. 2061-2067.
- [10] Huang, Y. and V. Yang. Dynamics and stability of lean-premixed swirl-stabilized combustion. Progress in Energy and Combustion Science, Vol. 35, 2009, pp. 293-364.
- [11] Dongbai, X., S. Guo, and D. Shi. Investigations on oxidation and microstructure evolution of pure Cu in simulated air-kerosene combustion atmospheres. Fire and Materials, Vol. 41, No. 6, 2016, pp. 614-624.
- [12] Boniardi, M. and A. Casaroli. In-depth approach to fire investigations: Microstructural analysis of metallic materials. Fire and Materials, Vol. 39, No. 6, 2015, pp. 600-618.
- [13] Dongbai, X., W. Wen, L. Shilei, and S. Guo. Effect of simulated combustion atmospheres on oxidation and microstructure evolution of aluminum alloy 5052. Fire and Materials, Vol. 42, No. 3, 2017, pp. 278-285.
- [14] Birks, N., G. H. Meier, and F. S. Pettit. Introduction to the high-temperature oxidation of metals, Cambridge University Press, New York, 2006.
- [15] Hao, H., D. B. Xie, and S. W. Duo. Effect of kerosene combustion atmosphere on surface oxide layer of low-carbon steel. Surface Technology, Vol. 49, No. 1, 2020, pp. 87-93.
- [16] Hong, H., D. Xie, S. Duo, and W. Wang. Investigating the oxidation behavior of carbon steel in fire scene: A new method

- for fire investigations. ScienceAsia, Vol. 46, No. 1, 2020, pp. 59-64.
- [17] Dongbai, X., S. Guo, and L. Shilei. Oxidation behavior of carbon steel in simulated kerosene combustion atmosphere: A valuable tool for fire investigations. Fire and Materials, Vol. 42, No. 2, 2017, pp. 156-163.
- [18] Xun, L. and L. Jixun. The oxidation of copper at 200-900°C. Acta Metallurgica Sinica, Vol. 8, No. 3, 1965, pp. 311-318.
- [19] Zhenhua, L., H. Yong, and C. Jun. The oxidation of pure copper in high heat. China Foundry Machinery & Technology, Vol. 6, 2011, pp. 11-13.
- [20] Darrell Ownby, P., X. Yang, and J. Liu. Calculated X-ray diffraction data for diamond polytypes. Journal of the American Ceramic Society, Vol. 75, No. 7, 1992, pp. 1876-1882.
- [21] Zhu, Y., K. Mimura, and M. Isshiki. Oxidation mechanism of Cu₂O to CuO at 600-1050°C. Oxidation of Metals, Vol. 62, No. 3/4, 2004, pp. 207-222.
- [22] Meishuan, L. High temperature oxidation of metals, Metallurgical Industry Press, Beijing, 2001, p. 45.
- [23] Gao, Z. C. and Z. Y. Wang. The mechanism of alcohol combustion reaction. Journal of Liaoning Technical University (Natural Science), Vol. 30, No. 1, 2003, pp. 63-66.
- [24] Li, J., A. Kazakov, and F. L. Dryer Dryer. Experimental and numerical studies of ethanol decomposition reactions. The Journal of Physical Chemistry A, Vol. 108, No. 38, 2004, pp. 7671-7680.
- Marinov, N. M. A detailed chemical kinetic model for high temperature ethanol oxidation. International Journal of Chemical Kinetics, Vol. 31, No. 3, 1999, pp. 183-220.
- [26] Saxena, P. and F. A. Williams. Numerical and experimental studies of ethanol flames. Proceedings of the Combustion Institute, Vol. 31, No. 1, 2007, pp. 1149-1156.
- [27] Pan, C., Y. Liu, F. Cao, J. Wang, and Y. Ren. Synthesis and growth mechanism of carbon nanotubes and nanofibers from ethanol flames. Micron, Vol. 35, No. 6, 2004, pp. 461-468.
- [28] Pan, C. and X. Xu. Synthesis of carbon nanotubes from ethanol flame. Journal of Materials Science Letters, Vol. 21, No. 15, 2002, pp. 1207-1209.
- [29] Liu, Y., Q. Fu, and C. Pan. Synthesis of carbon nanotubes on pulse plated Ni nanocrystalline substrate in ethanol flames. Carbon, Vol. 43, No. 11, 2005, pp. 2264-2271.
- [30] Dongbai, X., C. Jun, W. Zhen, D. Li, and T. Q. Zang. Effect of kerosene combustion atmosphere on corrosion of copper at high temperature. Corrosion Science and Protetion Technology, Vol. 28, No. 6, 2016, pp. 511-516.
- Dongbai, X. and S. Guo. Rapid identification of liquid accelerant in fire scene environment. Journal of Chinese Society for Corrosion and Protection, Vol. 37, No. 1, 2017, pp. 74-80.